electronics

MDPI

Article

Robust Sensor Fault Detection for a Single-Phase Pulse Width Modulation Rectifier

Egone Ndabarushimana * and Lei Ma *

School of Electrical Engineering, Southwest Jiaotong University, Chengdu 611756, China
* Correspondence: egone.ndabarushimana@ens.edu.bi (E.N.); malei@swjtu.edu.cn (L.M.)

Abstract: Maintaining safe and efficient operation in a single-phase pulse width modulation (PWM) rectifier that employs current sensors relies heavily on accurate sensor readings. However, several factors such as environmental conditions, aging, or damage can lead to sensor faults. Therefore, it is imperative to implement robust fault detection methods to ensure reliable system operation. The use of unknown input observer techniques is one such method that involves analyzing the differences between actual and estimated states to detect and identify faults in the system. This paper presents the development of a fault detection method that employs an unknown input observer with high sensitivity to faults and disturbance rejection to achieve robust fault detection. The method involves modeling the system as a state-space model and designing an observer to estimate the system's state variables based on input and output measurements. The deviations between the actual and estimated states are then analyzed to detect and identify sensor faults, without the need for additional hardware, making it a cost-effective solution. Hardware-in-the-loop tests confirm the effectiveness of the proposed method.

Keywords: single-phase PWM rectifier; fault detection; residual; unknown input observers

check for updates

Citation: Ndabarushimana, E.; Ma, L. Robust Sensor Fault Detection for a Single-Phase Pulse Width Modulation Rectifier. *Electronics* **2023**, *12*, 2366. https://doi.org/10.3390/electronics12112366

Academic Editors: Jose Luis Calvo-Rolle and Francisco Zayas-Gato

Received: 3 May 2023
Revised: 16 May 2023
Accepted: 19 May 2023
Published: 24 May 2023

1. Introduction

The need for higher performance, safety, and reliability in dynamic systems has led to an increased demand for fault diagnosis. However, a major challenge is to develop a fault detection method that can effectively detect faults while avoiding the impact of disturbances on the detection process. Critical systems such as power electronics converters are particularly susceptible to external perturbations that can interfere with fault detection. Therefore, there is a need to develop a robust fault detection method that can effectively handle such disturbances' impact.

Fault diagnosis research aims to develop techniques for detecting, isolating, and identifying faults in systems by analyzing sensor data, system behavior, or mathematical models [1]. The significance of fault diagnosis spans various applications. In industrial machinery and manufacturing, it ensures smooth operation, minimizes downtime, and improves productivity. In power systems and energy networks, it enhances grid stability and reduces equipment damage, such as gear fatigue [2]. In automotive systems, it enhances safety and performance, while in aerospace and aviation, it maintains aircraft reliability and safety. Additionally, fault diagnosis ensures accurate diagnostics and patient safety in medical equipment and healthcare. In renewable energy systems, it optimizes performance and efficiency, and in smart grid and Internet of Things (IoT) applications, it improves grid stability and resilience [3]. Overall, fault diagnosis prevents failures, reduces downtime, improves system reliability, and enables efficient resource allocation. Observer-based fault detection (FD) is a powerful tool for detecting faults in complex systems, such as aerospace and industrial applications, and it can significantly reduce downtime and maintenance costs [4]. Observer-based FD utilizes state/output observers that compare estimated system behavior with actual measurements to detect faults, while sensor detection specifically

focuses on identifying faults related to the sensors themselves. By employing specialized observers and filters, the system can accurately and reliably detect faults, even in the presence of noise or interference. This capability is particularly valuable in high-stakes applications where system failures can have severe consequences.

There are numerous fault detection methods available in the literature, each with its advantages and disadvantages. Among these methods, the unknown input observer (UIO) is a popular technique due to its simplicity and ability to detect faults without requiring additional hardware. However, to provide a clear comparison of critical factors, let us compare UIO with a few commonly used fault detection methods.

- Model-based approaches: Model-based approaches use mathematical models of the system to detect faults. These methods are often very accurate but require extensive knowledge of the system and its behavior under different fault conditions. Model-based approaches can be computationally expensive and may require additional hardware for fault detection [5];
- Residual-based methods: Residual-based methods compare measured and predicted system outputs to detect faults. These methods are less computationally expensive than model-based approaches but require accurate knowledge of the system's behavior and a precise model of the system. Residual-based methods may also suffer from the effects of disturbances, leading to false alarms or missed detections [6];
- Artificial intelligence-based methods: Artificial intelligence-based methods use machine learning algorithms to detect faults. These methods can learn complex patterns and may be more robust to disturbances than model-based or residual-based methods. However, they require large amounts of data to train the machine learning algorithms and may not be explainable, making it difficult to determine the cause of a detected fault [7].

Compared to these fault detection methods, the UIO technique has several advantages. UIO is a model-based approach that does not require any additional hardware for fault detection. It is computationally efficient and can detect faults quickly, allowing for faster maintenance and repair of the system. UIO is also less sensitive to disturbances than residual-based methods, reducing the likelihood of false alarms.

However, UIO does have limitations. It requires accurate knowledge of the system model, and its performance can be affected by modeling errors or uncertainty. Additionally, UIO is not suitable for detecting all types of faults and may require additional techniques to detect certain faults.

The use of unknown input observers for fault detection and identification has been widely studied in the control engineering literature. It was originally proposed by [8]. UIO is specifically designed to minimize the impact of disturbances, while still retaining a degree of sensitivity to faults. Using UIO is intended to enhance the reliability and accuracy of fault detection in systems that are prone to external interference or noise.

The potential application of UIO spans diverse systems, ranging from industrial control systems to automotive applications, where the assurance of the monitored system's reliability and safety necessitates fault detection and isolation [9]. UIO-based FDI techniques have been developed for various systems, including electrical, mechanical, and chemical systems. In [10], an adaptive UIO-based FDI approach was proposed for a wind turbines engine. The proposed approach used an adaptive gain matrix to estimate the unknown inputs and detect faults in the gas turbine engine. Ref. [11] presented a methodology to create unknown input observers that can estimate the state of a linear time-invariant dynamical system, taking into account both known and unknown inputs. This approach was applied to a physical hydraulic system to identify and pinpoint faults in the actuators. An UIO-based FDI approach was proposed for a wind turbine system in [12], where a linear matrix inequality (LMI) optimization technique has been used to design a UIO and generate a residual signal. The used strategy was shown to be effective in detecting and isolating faults while increasing the insensitivity to the noises. Ref. [13] expanded an algorithm for linear unknown input observer design to accommodate nonlinear systems by utilizing

unscented transformation (UT) to obtain the observer gain. This method is then applied to detect sensor faults in a highly nonlinear dynamic system, specifically the jacketed continuous stirred tank reactor (CSTR). A single full-order observer is devised to identify sensor faults in the presence of unknown. Through simulation results, it is demonstrated that the proposed method allows for differentiation between disturbances, which introduce model uncertainties, and the response caused by a sensor fault. The construction of UIOs for detecting unbalances in rotating systems has been presented in [14]. The design of observer matrices is based on the solution of LMIs and the algebraic Riccatti equation. A bank of observers is used to estimate the magnitude and axial position of unbalances and the simulation results are presented.

Robust sensor fault detection and identification based on UIO for a single-phase PWM rectifier is a specialized research topic that falls within the broader area of power electronics and control engineering. The disturbance decoupling based on the right eigenvector has been applied in [15], where the open circuit fault into the insulated gate bipolar transistor is considered. The study is limited to the actuator fault and the result is proved using simulation. In [16] the authors propose a fault detection and isolation method for a single-phase PWM rectifier based on Luenberger observers. The proposed method uses the observer to estimate the system state, and detect and isolate faults based on residual signal analysis. The detection of a fault occurrence in the transient and steady-state modes is achieved by monitoring the evolution of the generated residuals and their corresponding thresholds in [17]. Based on the pole placement strategy, [18] designed an observer able to detect and isolate the sensor fault in a single-phase PWM rectifier. However, the result presented using this method treated the DC-link sensor fault only and is limited to simulation. Ref. [19] proposes a fault diagnosis method for power electronics systems based on wavelet analysis and neural networks. The proposed method is tested on a DC-DC converter and shows an accurate diagnosis of faults.

Various fault detection techniques have been employed for insulated gate bipolar transistor (IGBT) systems, including mixed logical dynamic systems in [20], where a signal injection technique is used to excite the system and extract diagnostic features [21] presents an online fault diagnosis method that uses a modified phase-locked loop to estimate the rectifier output voltage and detect open-switch faults in the IGBTs of the rectifier. The proposed method is computationally efficient and can diagnose faults in real time. Robust sensor fault detection and isolation, and fault-tolerant control methods are presented by [22], and he used a state observer to estimate the system states, and a residual is generated to detect and isolate sensor faults. A fault-tolerant control strategy based on a sliding mode controller is then used to maintain the system performance in the presence of sensor faults. The proposed scheme is validated through simulation results, which show that the method can effectively detect and isolate sensor faults and maintain the system's performance. However, most of these techniques only focus on detecting and isolating open circuit faults and are limited to theoretical studies. Thus, the application of robust fault detection and identification remains an active area of research.

To meet the criteria for robustness, fault detection and isolation approaches that employ unknown input observers, eigenstructure assignment, and linear matrix inequalities (LMI) must satisfy three conditions, as noted in [23]:

(a) Amplifying the impact of faults on the residual;
(b) Stabilizing the gain observer;
(c) Decreasing the effects of disturbances on the residual.

This study's scientific novelty lies in its three key contributions as described below:

Firstly, the development of a highly sensitive unknown input observer approach that effectively detects faults while rejecting disturbances. This UIO technique generates a residual signal by comparing the actual current with the estimated current from the observer, without requiring any additional hardware.

Secondly, the proposed method is implemented for sensor fault detection on a single-phase pulse width modulation rectifier, which is a significant contribution to the field of fault detection in power electronics.

Thirdly, the effectiveness of the proposed method is validated through experimental testing using a hardware-in-the-loop (HIL) platform. The experimental test shows the accuracy and reliability of the proposed method in detecting faults and rejecting disturbances. Finally, the proposed method has the potential to significantly improve the accuracy of fault detection, reduce false alarms, and enhance the overall performance of the system.

The theory and design of the unknown input observer are summarized in Section 2 of this paper, and Section 3 outlines the experimental setup. Results and discussion are presented in Section 4, and this study concludes with Section 5.

2. Materials and Methods

2.1. Observer Design

System uncertainty can impact the dynamic system described by the equations in this section, and it can be expressed by an unknown disturbance term that is introduced to the system. This disturbance term can be considered a source of variability in the system's behavior that is difficult to predict or control. In other words, the uncertainty can introduce unexpected variations or errors in the system's output or performance, making it challenging to achieve the desired level of accuracy or stability. Therefore, it is crucial to account for and mitigate the effects of system uncertainty when designing or analyzing dynamic systems to ensure their reliable and robust operation. It is expressed by using the below equation:

$$\begin{cases} \dot{x}(t) = Ax(t) + Bu(t) + Ed(t) \\ y(t) = Cx(t) \end{cases} \tag{1}$$

The vectors x, u, and y refer to the state, input, and output of the system, respectively. The input disturbance is denoted by the letter $d(t)$.

The dimensions of matrices A, B, C, and E are known for a given system. E represents input distribution and should have a full column rank to ensure optimal system performance.

In the context of the system described by Equation (1), an observer can be considered an unknown input observer if it can estimate the state of the system accurately, despite the presence of input disturbances. The goal of the observer is to minimize the state estimation error vector $e(t)$, which ideally should converge to zero asymptotically.

In other words, the observer should be able to track the system's behavior and estimate its state accurately, even in the presence of disturbances. This ability is critical for ensuring reliable and robust system operation, especially in real-world applications where disturbances are common.

Therefore, the use of an unknown input observer is an effective technique for mitigating the effects of disturbances and improving the overall performance of dynamic systems [24]. By estimating the state of the system accurately, the observer can provide valuable information for control and optimization purposes, leading to better system behavior and increased efficiency. It is expressed by using the following equation:

$$\begin{cases} z(t) = \Gamma z(t) + B\Theta u(t) + Ky(t) \\ \hat{x}(t) = z(t) + \Pi y(t) \end{cases} \tag{2}$$

The estimated state vector $\hat{x} \in R^n$ and the state of the full-order observer $z \in R^n$ are related by certain matrices Γ, Π, Θ, and K that need to be designed for achieving unknown input decoupling and satisfying other design requirements.

By adopting the observer described in Equation (2) for the system described in Equation (1), the estimation error $e(t)$ can be calculated using Equation (3). This error quantifies the discrepancy between the estimated and actual states of the system and is influenced by various factors such as the system's dynamics and the quality of the input signals.

The design of the matrices Γ, Π, Θ, and K is critical for ensuring accurate state estimation and achieving the desired system performance. These matrices must be carefully chosen to meet the design requirements, such as unknown input decoupling, disturbance rejection, and robustness to noise.

The use of a full-order observer, such as the one described in Equation (2), can provide valuable insights into the system's behavior and help improve its performance. By estimating the system's states accurately, the observer can facilitate control and optimization strategies, leading to more efficient and effective system operation. The system with UIO is illustrated in Figure 1.

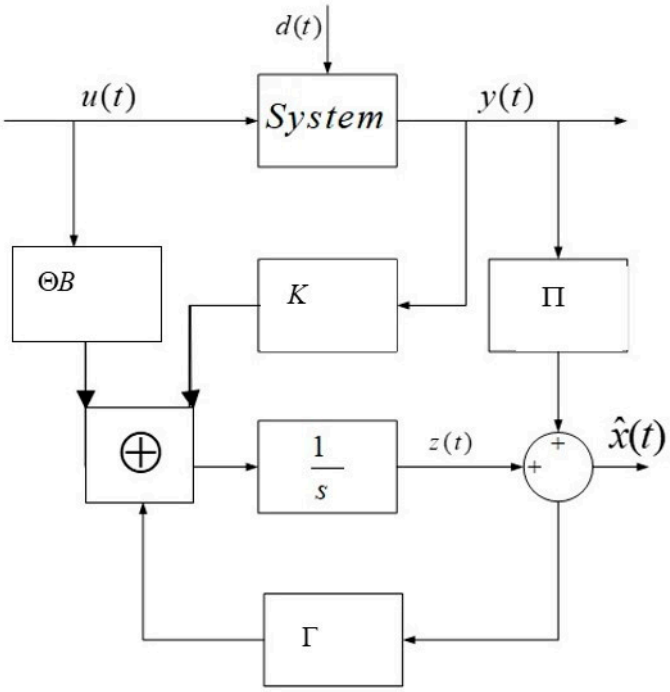

Figure 1. System with UIO scheme.

$$\dot{e}(t) = (A - \Pi CA - K_1C)e(t) + [\Gamma - (A - \Pi CA - K_1C)]z(t) + [K_2 - (A - \Pi CA - K_1C)\Pi]y(t) + [\Theta - (I - \Pi C)]Bu(t) + (\Pi C - I)Ed(t) \quad (3)$$

If the following relations are verified:

$$(\Pi C - I)E = 0 \quad (4)$$

$$\Theta = I - \Pi C \quad (5)$$

$$\Gamma = A - \Pi CA - K_1C \quad (6)$$

The state estimation error will then be:

$$\dot{e}(t) = Ne(t) \quad (7)$$

The estimation error $e(t)$ will converge to zero asymptotically, indicating that the observer functions as an unknown input observer, if all the eigenvalues of Γ are stable. To ensure the solvability of Equation (4), it is necessary to verify Equation (8).

The stability of the eigenvalues of Γ is critical for the observer's ability to estimate the system's states accurately and provide reliable information for control and optimization. A stable observer can effectively track the system's behavior, even in the presence of disturbances, and facilitate the achievement of design requirements such as disturbance rejection and robustness to noise.

Furthermore, verifying Equation (8) is essential for ensuring the solvability of Equation (4). The solvability of Equation (4) is necessary for accurate estimation of the system's states and

the effective functioning of the observer. If Equation (8) is not satisfied, Equation (4) cannot be solved, and the observer may not be able to estimate the system's states accurately.

Therefore, both the stability of the eigenvalues of Γ and the verification of Equation (8) are crucial for the design and implementation of effective unknown input observers, which can provide valuable insights into the behavior of dynamic systems and enhance their performance.

$$rank(CE) = rank(E) \tag{8}$$

For Equation (2) to function as an unknown input observer, an additional requirement is that the pair (C, A_1) should be detectable. This means that the system's output C and its state dynamics A should be observable, allowing for accurate estimation of the system's states using the observer.

Detectability is an important property of dynamic systems that ensures the availability of sufficient information for state estimation and control. If (C, A_1) is detectable, the observer can effectively estimate the system's states, even in the presence of unknown inputs or disturbances. This ability is crucial for achieving robust and reliable system performance, especially in real-world applications where disturbances and uncertainties are common.

Therefore, the detectability of the pair (C, A_1) is a critical design requirement for the development of effective unknown input observers, which can provide valuable insights into the behavior of dynamic systems and help improve their performance. Let's compute:

$$A_1 = A - E[(CE)^T CE]^{-1}(CE)^T CE \tag{9}$$

By defining the solution for Π as $\Pi^* = E[(CE)^T CE]^{-1}(CE)^T$, the dynamic matrix Γ can be written as:

$$\Gamma = A - \Pi CA - K_1 C = A_1 - K_1 \mathrm{C} \tag{10}$$

To stabilize Γ, one can choose K_1 such that the second condition is satisfied. The pole-placement method can be used to design K_1, which involves selecting the closed-loop poles of the system to achieve a desired response.

By choosing appropriate values for K_1, the system's stability can be ensured, leading to accurate state estimation and robust system performance. The pole-placement method is a widely used technique in control engineering and is known for its effectiveness in achieving stable and responsive systems.

The design of K_1 is a crucial step in developing an effective unknown input observer, which can provide valuable information about the behavior of dynamic systems and help optimize their performance. By carefully selecting the closed-loop poles, one can achieve the desired response and ensure that the system is stable and reliable, even in the presence of disturbances or uncertainties.

Therefore, the use of the pole-placement method to design K_1 is an important design consideration for the development of effective unknown input observers, which can enhance the performance of dynamic systems in various real-world applications.

A comprehensive guide on the design of UIOs can be found in [24]. The following algorithm outlines the steps involved in designing an unknown input observer:

(1) *Verify whether the rank of (CE) is the same as the rank of (E); if not, the UIO cannot be established and the process should be halted.*
(2) *Calculate* Π, Θ *and A1.*
(3) *Determine whether the pair (C, A1) is observable; if it is observable, the UIO can be created, and K1 can be found using pole placement. The process can be stopped at this point.*
(4) *Create a transformation matrix P for the observable canonical decomposition: choose the independent* $n_1 = rank(w_0)$*, where* w_0 *is the observability matrix of* (C, A_1)*, row vector* $p_1^T, \ldots, p_{n1}^T$ *from* w_0*, together with other* $n - n_1$ *row vectors* $p_{n1+1}^T, \ldots, p_n^T$ *to construct a non-singular matrix as:* $P = [p_1, \ldots, p_{n0}; p_{n0+1}, \ldots, p_n]^T$.

(5) *Create an observable canonical decomposition on* (C, A_1)*:*$PA_1P^{-1} = \begin{bmatrix} A_{11} & 0 \\ A_{21} & A_{22} \end{bmatrix} CP^{-1} = [C^* \quad 0]$.

(6) *Verify if (C, A1) is detectable: if any one of the eigenvalues of* A_{22} *is unstable the UIO cannot be established and the process should be halted.*

(7) *Choosen*$_1$ *desired eigenvalues and assign them to* $A_{11} - K_p^1 C^*$.

(8) *Calculate* $K_1 = P^{-1}K_p = P^{-1}[(K_p^1)^T \ (K_p^2)^T]^T$ *where* K_p^2 *is any* $(n - n_1)\times$ *matrix.*

(9) *Compute* Γ *and K:*

$$\Gamma = A_1 - K_1 C$$
$$K = K_1 + K_2 = K_1 + \Gamma\Pi$$

(10) *Stop*

After designing the UIO, the description of the robust residual is as follows:

$$r(t) = y(t) - C\hat{x}(t) = (I - C\Pi)y(t) - Cz(t) \tag{11}$$

The method described in the previous section can be applied to rectifiers, and to do so, it is necessary to first establish the rectifier's state space description. This description provides a mathematical representation of the rectifier's behavior and allows for the application of control and estimation techniques to improve its performance.

The state space description of a rectifier is typically formulated using a set of differential equations that relate the rectifier's input, output, and internal states. This set of equations can be organized in matrix form, where the rectifier's state vector represents the internal states, and the input and output vectors capture the rectifier's behavior in response to external stimuli.

By establishing the rectifier's state space description, it becomes possible to apply the method described in the previous section to estimate the rectifier's internal states and improve its performance. This can involve the design of a UIO, as well as the application of control techniques to regulate the rectifier's output and ensure stable operation.

2.2. Description Rectifier System

To model the analyzed system, the state equations presented below are utilized. These equations consider the binary switching control signal S and assume that the dead time can be ignored.

$$\begin{cases} U_n = -L\frac{di_c}{dt} - Ri_c + U_{ab} \\ i_{cd} = C_{cd}\frac{dV_{dc}}{dt} \\ i_{dc} = i_{cd} + i_{ld} \end{cases} \tag{12}$$

Figure 2 illustrates the various currents and voltages present in the system, where i_c represents the catenary current, i_{cd} denotes the capacitor current, and i_{ld} represents the load current. The grid voltage is denoted as U_n, and the DC-link voltage is represented as V_{dc}. The output converter current is denoted as i_{dc}, while the input rectifier voltage is expressed by U_{ab} and is defined in Equation (13).

$$\begin{cases} U_{ab} = (2S - 1)V_{dc} \\ i_{dc} = -(2S - 1)i_c \end{cases} \tag{13}$$

Equation (14) presents the state space model of the rectifier in the presence of uncertainties. This equation can be derived by obtaining Equations (10) and (11)

$$\begin{cases} x(t) = [A(t) + \Delta A(v,t)]x(t) + [B(t) + \Delta B(v,t)]u(t) + E(t)d(t) \\ y(t) = C(t)x(t) \end{cases} \tag{14}$$

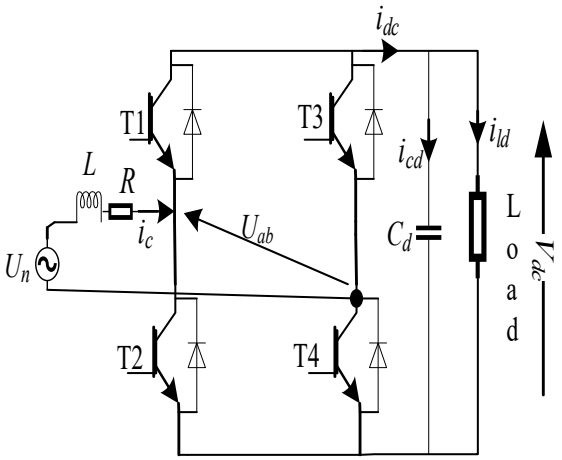

Figure 2. Schematic of single-phase PWM rectifier [25].

The system matrices $A(t), B(t)$ and $C(t)$ are constants with $\Re e[\lambda\ (A)] \prec 0$, and designed as:

$$A = \begin{bmatrix} -\frac{R}{L} & \frac{2S-1}{L} \\ \frac{-2S+1}{C_d} & 0 \end{bmatrix}, B = \begin{bmatrix} -\frac{1}{L} \\ 0 \end{bmatrix}, C = \begin{bmatrix} 1 & 0 \\ 0 & 1 \end{bmatrix} \tag{15}$$

The IGBT's switching control signal, denoted as S, has two logical states of 1 or 0. As a result, matrix A in the system's state space model also has two distinct expressions within a single switching period, which are presented below.

$$A_{s=0} = \begin{bmatrix} -\frac{R}{L} & \frac{-1}{L} \\ \frac{1}{C_d} & 0 \end{bmatrix}, A_{s=1} \begin{bmatrix} -\frac{R}{L} & \frac{1}{L} \\ \frac{-1}{C_d} & 0 \end{bmatrix} \tag{16}$$

$$\begin{cases} x = \begin{bmatrix} i_c & V_{dc} \end{bmatrix}^T \\ u = U_n \end{cases} \tag{17}$$

If we assume that the perturbation only impacts the control vector, it becomes possible to regulate the distribution matrix of the disturbance input through the use of matching conditions. Based on the theory presented in [26], the following assumptions are made:

Assumption 1. $\{A(.), B(.)\}$ *completely controllable in a uniform manner.*

Assumption 2. *For all* $(x, t) \in \Re^n \times \Re$, *there exist matrix functions* $O(.), Q(.), D(.)$ *with dimensions that are suitable and continuous:*

$(a)\ \Delta A(v,t) = B(t)O(v,t)$
$(b)\ \Delta B(v,t) = B(t)Q(v,t)$.
$(c)\ E(t) = B(t)D(t)$

In the given system, the system uncertainty matrices $\Delta A(.)$ and $\Delta B(.)$ are continuous across all their arguments, while the vectors v and v are uncertain. The variation in system parameters is dependent solely on R, C_d, and L (refer to Figure 2). It is assumed that the variation in C_d can be ignored, and if there is a 1% variation in each parameter, then Equation (18) can be obtained as follows:

$$\begin{cases} \Delta A(t) = \begin{bmatrix} |\Delta a_{11}| & |\Delta a_{12}| \\ 0 & 0 \end{bmatrix} = \begin{bmatrix} 0.230 & 4.34780 \\ 0 & 0 \end{bmatrix} \\ \Delta B(t) = \begin{bmatrix} |\Delta b_{11}| \\ 0 \end{bmatrix} = \begin{bmatrix} 4.34780 \\ 0 \end{bmatrix} \end{cases} \tag{18}$$

Assumption 1 states that matching conditions, which are inherent to the system's structure, ensure that the dynamics are minimally affected by the uncertainty vector in comparison to the control vector u [27].

If conditions (a) and (b) are met, the structure of Equation (1) becomes as follows:

$$\begin{cases} \dot{x}(t) = A(t)x(t) + B(t)[(u(t) + \eta(v, v, t] \\ y(t) = C(t)x(t) \end{cases} \tag{19}$$

where $\eta = O(.)x(t) + Q(.)u(t) + D(.)d(t)$.

As stated in Assumption 1, this suggests that the dynamics of the system are impacted by the control vector u to a greater extent than by the uncertainty vector η. The equation provided in this section satisfies the matching conditions for the PWM rectifier system under consideration

$$O = \begin{bmatrix} -0.005290 & -0.010 \end{bmatrix};\ Q = -0.01;\ D = 1.0$$

Following that, the design of UIO for the converter system is required, which should be based on the system equations. By using Assumption 2 and Equation (19), we can formulate the following expression: $E = B$, so the rank of the matrix (CE) is equal to the rank of the matrix E.

Having verified the first necessary condition, we can proceed to the second step, which involves designing the matrices Θ, Π, and A_1. Table 1 presents different parameter values related to the system and the load used in this work is equal 20Ω.

Table 1. Parameters for the rectifier used.

Parameters	Symbols	Values	Unity
Filter resistor	R	0.530	Ω
Filter inductor	L	$23e^{-4}$	H
DC-link capacitor	C_d	$80e^{-4}$	F
Grid voltage	U_n	1550	V
DC-link voltage	V_{dc}	3000	V
Rectifier switching frequency	f_s	1250	Hz

$$\Pi = \begin{bmatrix} 1 & 0.001 \\ 0 & -0.499 \end{bmatrix}; \Theta = \begin{bmatrix} 0 & -0.001 \\ 0 & 1.499 \end{bmatrix}, A_1 = \begin{bmatrix} -0.1206 & 0 \\ 187.37 & 0 \end{bmatrix}$$

Confirmation of the necessary conditions for the existence of the UIO is provided by the observability of the pair (C, A_1). This enables us to calculate the K_1 and then derive the Γ and K matrices accordingly.

$$K_1 = \begin{bmatrix} 24.87940 & 0 \\ 187.3750 & 26 \end{bmatrix}, \Gamma = \begin{bmatrix} -25 & 0 \\ 0 & -26 \end{bmatrix}$$
$$K_2 = \begin{bmatrix} -25 & -0.02410 \\ 0 & 12.9740 \end{bmatrix}; K = \begin{bmatrix} -0.12060 & -0.02410 \\ 187.3750 & 38.9740 \end{bmatrix}$$

The pole placement has been used to generate K_1, whit $p = \begin{bmatrix} -25 & -26 \end{bmatrix}$.

The robust residual designed in this manner enables the detection of faults using a simple threshold logic, as follows:

$$\begin{cases} r < Threshold: \ no\ fault \\ r > Threshold: there\ is\ a\ fault \end{cases} \tag{20}$$

3. Experimental Setup

The proposed Unknown Input Observer technique was tested for its effectiveness and validity through experimental validation on a hardware-in-the-loop platform, which is

shown in Figure 3. The test setup comprised two personal computers: one was used for the dSPACE software, and the other for code composer studio programming. In addition to these, a DSP control board (TMS320F28335), a real-time simulator for dSPACE, and an oscilloscope were utilized to display signal waveforms and act as the information interface. The analog signals were received by the DSP from the dSPACE simulator, and after undergoing analog-to-digital conversion and computation, the control signals for the switching devices were delivered.

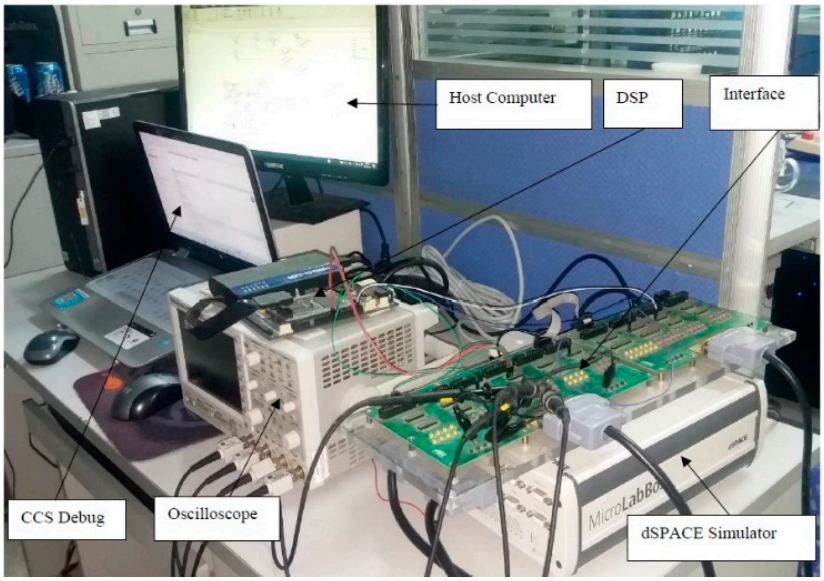

Figure 3. Experimental test setup platform.

The control algorithm program for the single-phase PWM rectifier was developed using code composer studio and downloaded onto the DSP board. The experimental validation demonstrated the efficacy of the UIO technique, as the signals displayed on the oscilloscope were consistent with the expected waveforms. The use of the hardware-in-the-loop platform enabled the testing of the UIO technique in a realistic and dynamic environment, allowing for a more accurate assessment of its effectiveness. The experimental validation thus confirmed the validity and applicability of the proposed UIO technique in practical implementations.

4. Results and Discussion

To achieve a unity power factor operation and regulate the DC-link voltage in a single-phase PWM rectifier, a control strategy that employs a proportional integrator (PI) controller in the external control loop and a proportional resonant (PR) controller in the inner loop control is adopted. The details on this controller design can be found in [28].

The PI controller in the external control loop serves to regulate the DC-link voltage by adjusting the output voltage of the rectifier. This is done by comparing the actual DC-link voltage to the reference voltage selected equal to 3000 V, and the resulting error signal is fed into the PI controller. The PI controller then calculates the required adjustment to the output voltage, which is then used to adjust the pulse width of the switching signals.

In the inner loop control, a PR controller is employed to regulate the output current of the rectifier. The PR controller is designed to track the reference current signal and suppress any harmonics that may be present in the system. This is done by decomposing the current signal into its fundamental and harmonic components and applying the proportional resonant controller to the harmonic component to eliminate it. The result depicted in Figure 4 demonstrates the effectiveness of the adopted controller in normal operation. The trace denoted V_{dc} represents the DC-link voltage, the trace U_n is the input grid voltage signal, i_c represents the actual signal of the current from the sensor, and the trace i_{c_est}

represents the estimated current of the actual current and is from the observer. The trace *r* and *Th* represent the residual signal and the detection threshold, respectively.

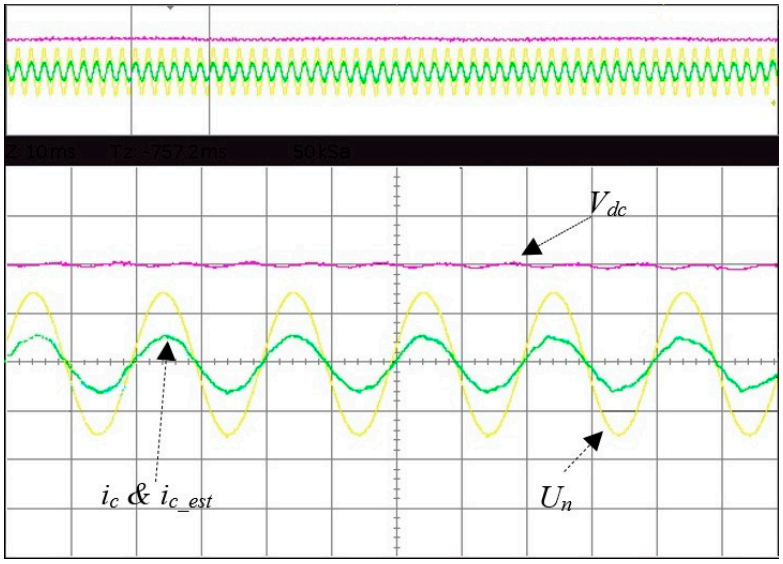

Figure 4. Input and output signals before the faults occur (U_n [1.572 KV/div.], i_c and i_{c_est} [0.834 KA/div], V_{dc} [1.5 KV/div], time [10 ms/div]).

To evaluate the effectiveness of the proposed method in separating disturbances, a white noise signal with a noise power of 10 was added to the input voltage before inducing faults. The residual performance was examined during the presence of noise, as shown in Figure 5. The results revealed that the residual behavior remained unchanged despite the addition of disturbances, indicating the effectiveness of the proposed method in decoupling disturbances. Compared to [29,30] where the evaluation of the impact of disturbance has been ignored by the authors, this practice is the most important when designing a robust fault detection. These results are significant as they demonstrate the feasibility of using the proposed method in practical applications, where systems are typically subject to various disturbances and noise.

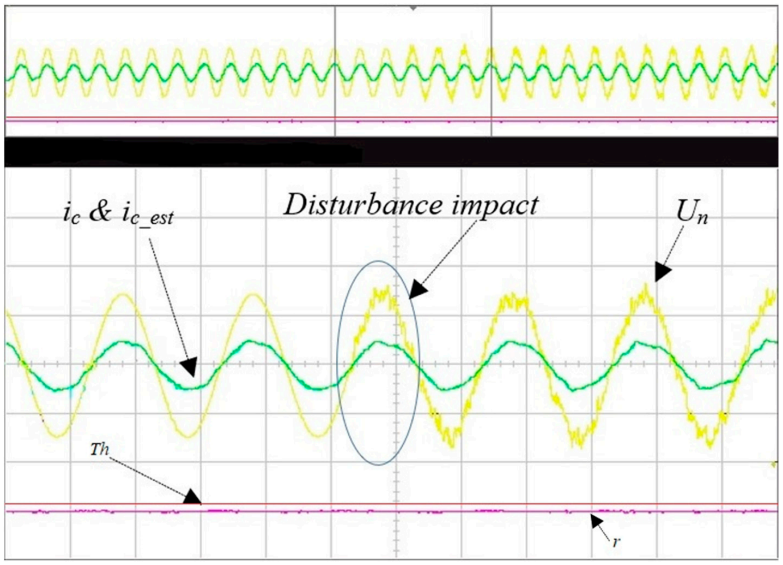

Figure 5. Impact of disturbances on the system (U_n [1.572 KV/div.], i_c and i_{c_est} [0.834 KA/div], time [10 ms/div]).

After successfully testing the ability of the proposed method in disturbance decoupling, we moved on to evaluate its ability in fault detection. To simulate a fault, we introduced a signal with a frequency of 50 Hz and an amplitude of 30 into the electric current sensor signal using a signal generator available in Simulink at a specific time, as depicted in Figure 6.

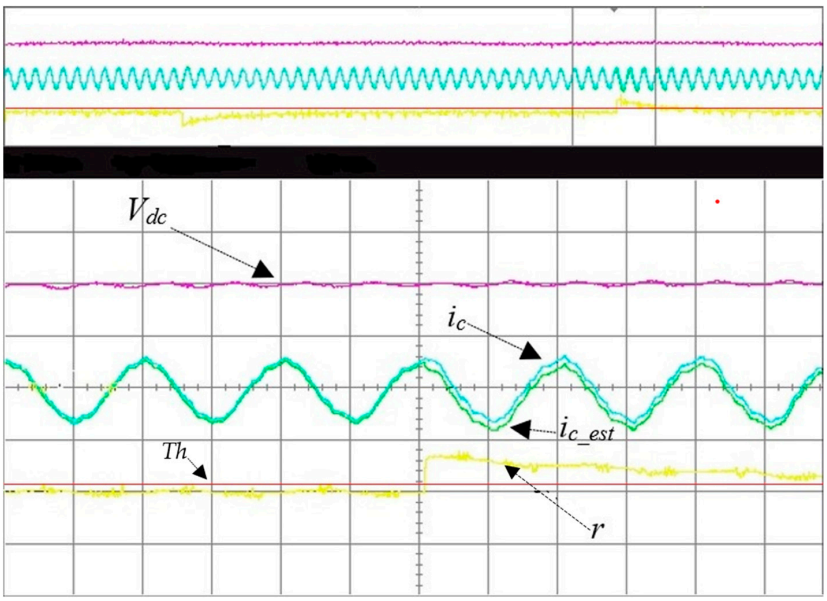

Figure 6. Measured current, estimated current (i_{c_est}), residual (r [10 A/div]) signals' behavior after the faults occur. Threshold (Th [10 A/div]), time [10 ms/div].

The experimental results showed that the measured and estimated electric current signals were aligned and merged before the plant was affected by the fault, indicating that the designed control strategy was effective in normal operation. However, once the fault was introduced into the system, there was a significant divergence between the estimated and measured electric current signals, leading to a noticeable gap between them, as shown in Figure 6.

To detect the fault, we utilized the difference between the estimated and measured current to generate a residual signal, as seen in Figure 6, and the residual signal is compared to the selected detection threshold (noted Th) equal to 1.9 A. The selection of the detection threshold is based on the observation of the residual signal behavior in normal operation. The fault detection is made based on the algorithm given in Equation (20). It can be seen in Figure 6 that the residual signal amplitude exceeds the detection threshold with a time shorter than 1 ms after the fault is induced. This time is more than enough to prevent the second fault and is the best when compared with the response time of 3 ms obtained by [20]. It also proves the sensitivity of the generated residual on the fault, which is good in the fault detection process. This sensitivity is crucial for effective fault detection.

5. Conclusions

A reliable unknown input observer technique for detecting faults in single-phase pulse width modulation rectifiers has been developed successfully. This method utilizes the difference between actual and estimated current to generate a residual for fault detection, without requiring any additional hardware. With only the measured current, DC-link voltage, and grid voltage available, this technique is cost-effective and easy to implement. It is highly reliable, with fast diagnosis and a detection time of less than 2 ms, allowing for the avoidance of secondary faults in other components, and improving overall reliability and efficiency. Experimental testing on a hardware-in-the-loop platform has validated the effectiveness and accuracy of this approach by demonstrating its potential for use in

real-world fault detection applications. By decoupling disturbances, the proposed method significantly reduces the likelihood of false alarms, enhancing the overall performance of the system. Therefore, the effectiveness of this approach in isolating faults and decoupling disturbances makes it a promising candidate for practical implementation.

Research Limitation:

The present study focuses on the current sensor fault while neglecting the study of DC-link voltage sensor fault by using an unknown input observer to detect the faults and decouple disturbances. Although the proposed method addressed one aspect of sensor faults, a comprehensive analysis incorporating both current and DC-link voltage sensor faults would provide a more complete understanding of the system's fault diagnosis capabilities.

Potential Improvement for Future Works:

In future research, it is recommended to extend the investigation to encompass both current and DC-link voltage sensor faults. This expansion will enhance the proposed method's robustness and effectiveness in fault diagnosis. By incorporating fault detection and isolation techniques for both sensors, the system will have a more comprehensive fault diagnosis framework. Furthermore, to ensure system resilience in the presence of sensor faults, future works should explore fault-tolerant control strategies. The integration of fault diagnosis and fault tolerant control will enable the system to maintain stable operation and mitigate the impact of sensor faults on overall performance. Conducting such studies will contribute to the development of more advanced and reliable fault diagnosis techniques for practical applications.

Author Contributions: The study's design and development benefited from the work of all the writers. The information was created, the data was gathered, and the analysis was completed by E.N. The first draft of the paper was written by E.N., while L.M. provided comments on earlier revisions. The final draft was reviewed and approved by all authors. Before submission, this manuscript was evaluated by L.M. All authors have read and agreed to the published version of the manuscript.

Funding: This study's funding was provided by the Chinese National Science Foundation under grant number 61733015.

Data Availability Statement: Upon a reasonable request, the relevant author will make the datasets created during the current inquiry available. Any researcher wishing to use the resources offered in the paper for non-commercial endeavors without jeopardizing participant confidentially is free to access all pertinent raw data.

Conflicts of Interest: The authors assert that there were no conflict of interest or strong personal links that would have looked to affect the research revealed in this study.

References

1. Yan, W.; Wang, J.; Lu, S.; Zhou, M.; Peng, X. A Review of Real-Time Fault Diagnosis Methods for Industrial Smart Manufacturing. *Processes* **2023**, *11*, 369. [CrossRef]
2. Feng, K.; Ji, J.C.; Ni, Q. A novel gear fatigue monitoring indicator and its application to remaining useful life prediction for spur gear in intelligent manufacturing systems. *Int. J. Fatigue* **2023**, *168*, 107459. [CrossRef]
3. Abid, A.; Khan, M.T.; Iqbal, J. A review on fault detection and diagnosis techniques: Basics and beyond. *Artif. Intell. Rev.* **2021**, *54*, 3639–3664. [CrossRef]
4. Isermann, R. Model-based fault-detection and diagnosis—Status and applications. *Annu. Rev. Control* **2005**, *29*, 49–60. [CrossRef]
5. Hwang, I.; Kim, S.; Kim, Y.; Seah, C.E. A Survey of Fault Detection, Isolation, and Reconfiguration Methods. *IEEE Trans. Control Syst. Technol.* **2010**, *18*, 636–653. [CrossRef]
6. Miljkovic, D. Fault detection methods: A literature survey. In Proceedings of the 2011 Proceedings of the 34th International Convention MIPRO, Opatija, Croatia, 23–27 May 2011.
7. Zhao, Y. Artificial intelligence-based fault detection and diagnosis methods for building energy systems_ Advantages, challenges and the future. *Renew. Sustain. Energy Rev.* **2019**, *109*, 85–101. [CrossRef]
8. Chen, J.; Zhang, H. Robust detection of faulty actuators via unknown input observers. *Int. J. Syst. Sci.* **1991**, *22*, 1829–1839. [CrossRef]
9. Frank, P.M. Robust Model-Based Fault Detection in Dynamic Systems. *IFAC Proc. Vol.* **1992**, *25*, 1–13. [CrossRef]
10. Li, C.; Teng, J.; Yang, T.; Feng, Y. Adaptive observer based fault detection and isolation for winds turbines. In Proceedings of the 2020 Chinese Automation Congress (CAC), Shangai, China, 6–8 November 2020; pp. 481–486. [CrossRef]

11. Gaddouna, B.O.; Ouladsine, M. Fault diagnosis in a hydraulic process using unknown input observers. In Proceedings of the 1997 IEEE International Conference on Control Applications, Hartford, CT, USA, 5–7 October 1997; pp. 490–495. [CrossRef]
12. Madubuike, K.; Mayhew, C.; Zhang, Q.; Gomm, B.; Yu, D.-L. Fault diagnosis for wind turbine systems using unknown input observer. In Proceedings of the 2019 25th International Conference on Automation and Computing (ICAC), Lancaster, UK, 5–7 September 2019; pp. 1–6. [CrossRef]
13. Zarei, J.; Poshtan, J. Design of Nonlinear Unknown Input Observer for Process Fault Detection. *Ind. Eng. Chem. Res.* **2010**, *49*, 11443–11452. [CrossRef]
14. Ambur, R.; Vadamalu, R.S.; Rinderknecht, S. Identification of unbalance faults in rotors with unknown input observers using classical and LMI based approaches. In Proceedings of the 2016 European Control Conference (ECC), Aalborg, Denmark, 29 June–1 July 2016; pp. 1904–1908. [CrossRef]
15. Egone, N.; Ma, L.; Qin, N. Disturbance De-coupling for Faults Detection and Identification Based on Right Eigenvectors Assignment for a Single-phase PWM Rectifier. In Proceedings of the 2020 39th Chinese Control Conference (CCC), Shenyang, China, 27–29 July 2020; pp. 4048–4053. [CrossRef]
16. Xu, T.; Jiang, B. Sensor fault detection and diagnosis for a three-phase PWM rectifier using wavelet analysis and adaptive observer. *IEEE Trans. Power Electron.* **2013**, *28*, 4433.
17. Jlassi, I.; Estima, J.O.; El Khil, S.K.; Bellaaj, N.M.; Cardoso, A.J.M. A Robust Observer-Based Method for IGBTs and Current Sensors Fault Diagnosis in Voltage-Source Inverters of PMSM Drives. *IEEE Trans. Ind. Appl.* **2017**, *53*, 2894–2905. [CrossRef]
18. Kavinelavu, K.; Kalaivani, S. Pole placement-based sensor fault detection and isolation of a single phase PWM rectifier for electric railway traction. In Proceedings of the 2014 International Conference on Computation of Power, Energy, Information and Communication (ICCPEIC), Chennai, India, 16–17 April 2014; pp. 194–199. [CrossRef]
19. Gao, L.; Li, H.; Wang, H. Fault diagnosis of power electronics systems using wavelet analysis and neural network. *IEEE Trans. Ind. Electron.* **2003**, *50*, 757–767.
20. Gou, B.; Ge, X.-L.; Wang, S.; Feng, X. An open-switch fault diagnosis method for single-phase PWM rectifier using a model-based approach in high-speed railway electrical traction drive system. *IEEE Trans. Power Electron.* **2016**, *31*, 3816–3826. [CrossRef]
21. Ge, X.-L.; Liu, Y.-C.; Pu, J.-K. Online open-switch fault diagnosis method in single-phase PWM rectifiers. *Electron. Lett.* **2015**, *51*, 1920–1922. [CrossRef]
22. Ben, A.; El Khil, S.K.; Slama-Belkhodja, I. State observer-based sensor fault detection and isolation, and fault tolerant control of single-phase PWM rectifier for electric railway traction. *IEEE Trans. Power Electron.* **2013**, *28*, 12.
23. Zhang, Y.; Polycarpou, M.; Liu, F. Observer-based Fault Detection and Diagnosis: State-of-the-Art and Applications. *IEEE Trans. Control Syst. Technol.* **2005**, *13*, 549–558.
24. Chen, J.; Patton, R.J.; Chen, J.; Patton, R.J. *Robust Model-Based Fault Diagnosis for Dynamic Systems*; Kluwer: Norwell, MA, USA, 1999.
25. Egone, N.; Ma, L.; Qin, N. Faults Detection and Identification Based on Robust Residual Generation for A Single-Phase PWM Rectifier. In Proceedings of the 2019 IEEE 3rd Conference on Energy Internet and Energy System Integration (EI2), Changsha, China, 8–10 November 2020. [CrossRef]
26. Gutman, S. Uncertain Dynamical Systems-A Lyapunov Min-Max Approach. *IEEE Trans. Autom. Control* **1979**, *24*, 437–443. [CrossRef]
27. Cheres, E.; Gutman, S.; Palmor, Z.J. Stabilization of Dynamic systems including state delay. *IEEE Trans. Autom. Control* **1989**, *34*, 1199–1203. [CrossRef]
28. Qin, H.; Kimball, J.W. Closed-Loop Control of DC–DC Dual-Active-Bridge Converters Driving Single-Phase Inverters. *IEEE Trans. Power Electron.* **2014**, *29*, 1006–1017. [CrossRef]
29. Xian, Y.; Xu, Y.; Gou, B. Current sensor fault diagnosis and fault tolerant control for single-phase PWM rectifier based on a hybrid model-based and data driven method. *IET Power Electron.* **2020**, *13*, 4150–4157. [CrossRef]
30. Gong, Z.; Huang, D.; Jadoon, H.U.K.; Ma, L.; Song, W. Sensor-Fault-Estimation-Based Tolerant Control for Single-Phase Two-Level PWM Rectifier in Electric Traction System. *IEEE Trans. Power Electron.* **2020**, *35*, 12274–12284. [CrossRef]